JACS
JOURNAL OF THE AMERICAN CHEMICAL SOCIETY

ARTICLE

pubs.acs.org/JACS

Spatiotemporal Multicolor Labeling of Individual Cells Using Peptide-Functionalized Quantum Dots and Mixed Delivery Techniques

James B. Delehanty,*[,†] Christopher E. Bradburne,[†] Kimihiro Susumu,[‡] Kelly Boeneman,[†] Bing C. Mei,[‡] Dorothy Farrell,[‡] Juan B. Blanco-Canosa,[§] Philip E. Dawson,[§] Hedi Mattoussi,[‡,∥] and Igor L. Medintz*[,†]

[†]Center for Bio/Molecular Science and Engineering, and [‡]Optical Sciences Division, U.S. Naval Research Laboratory, Washington, DC 20375, United States

[§]The Scripps Research Institute, La Jolla, California 92037, United States

Supporting Information

ABSTRACT: Multicolor fluorescent labeling of both intra- and extracellular structures is a powerful technique for simultaneous monitoring of multiple complex biochemical processes. This approach remains extremely challenging, however, as it often necessitates the combinatorial use of numerous targeting probes (e.g., antibodies), multistep bioconjugation chemistries, different delivery strategies (e.g., electroporation or transfection reagents), cellular fixation coupled with membrane permeabilization, and complex spectral deconvolution. Here, we present a nanoparticle-based fluorescence labeling strategy for the multicolor labeling of distinct subcellular compartments within live cells without the need for antibody conjugation or cellular fixation/permeabilization. This multipronged approach incorporates an array of delivery strategies, which localize semiconductor quantum dots (QDs) to various subcellular structures. QD uptake is implemented in a spaciotemporal manner by staggering the delivery of QD−peptide composites and exploiting various innate (peptide-mediated endocytosis, peptide−membrane interaction, polymer-based transfection) along with physical (microinjection) cellular delivery modalities to live cells growing in culture over a 4 day period. Imaging of the different intracellular labels is simplified by the unique photophysical characteristics of the QDs in combination with Förster resonance energy transfer sensitization, which allow for multiple spectral windows to be accessed with one excitation wavelength. Using this overall approach, QDs were targeted to both early and late endosomes, the cellular cytosol, and the plasma membrane in live cells, ultimately allowing for simultaneous five-color fluorescent imaging.

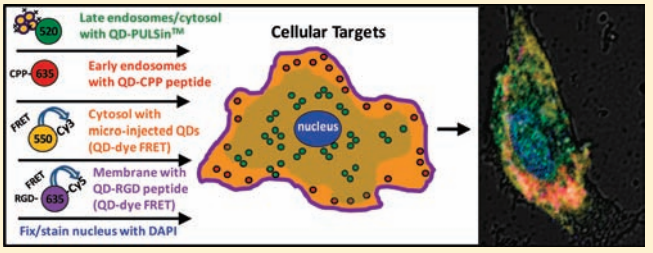

INTRODUCTION

The fluorescent labeling of cells is a fundamental technology in both basic biology and medical diagnostics as it allows for the visualization of organelles as well as the real-time monitoring of biochemical processes in vivo.[1] Achieving complex multicolor fluorescent labeling within the same cells is an important continuing goal as it can allow the spaciotemporal correlation of coordinated biological processes.[1−4] This goal continues to be hampered by two issues: the physiochemical liabilities of traditional organic dyes and achieving the requisite and robust site-specific delivery and labeling of subcellular structures. Organic dyes can suffer from photoinstability, pH and ionic sensitivity, susceptibility to chemical degradation, low quantum yields (QYs), and solubility issues.[5,6] When applied to multiplex formats, the broad overlapping absorption and emission profiles of such dyes often require multiple excitation sources coupled with complicated deconvolution analysis.[7] Specific labeling of cellular organelles in a multicolor format is most often achieved using differentially labeled primary and/or secondary antibodies. Because of their relatively large size (≥150 kD) and cell impermeability, the probing of intracellular targets with antibodies requires prior cellular fixation and permeabilization. As a result, it is not readily amenable to live cell labeling of intracellular structures. Further, as antibodies have a high propensity to cross-react with each other, multicolor labeling formats also require careful pretesting and selection of a viable working set for a particular combination of cellular targets.[8,9]

Continuing development of new fluorophores such as long-lifetime chelates, metallic nanocrystals, nanoparticles (NPs), and fluorescent proteins has provided an expanding menu of fluorophores for multicolor labeling with optical properties that can potentially overcome some of the aforementioned issues.[1,5,6,10−13] Semiconductor quantum dot (QD) properties in particular appear to be well-suited for multiplexing applications.[10−13] Relevant photophysical characteristics include size-tunable narrow-symmetric photoluminescence (PL) spanning from the UV to near-IR, high QYs, large

Received: January 19, 2011
Published: May 31, 2011

effective Stokes shifts, strong chemical/photostability, some of the largest two-photon action cross sections available, which permit relatively deep-tissue imaging, and, most importantly, the ability to excite multiple QD populations at one wavelength significantly blue-shifted from their respective emissions. These properties have also made them useful as Förster resonance energy transfer (FRET) donors.[6,12] QDs also contribute relatively small sizes, which are commonly on the order of <10 nm hard diameter and <25 nm hydrodynamic diameter, availability of multiple bioconjugation chemistries, along with the ability to be functionalized with multiple copies of the same or different biomolecular species providing access to higher avidity interactions.[6,10−13]

In a similar vein, the development of potent cell penetrating peptides (CPPs) and other transfection reagents has also provided numerous methods by which to achieve delivery of protein, drug, and especially nanoparticle cargos to cells.[14−16] These delivery technologies in conjunction with the growing availability of QDs have allowed them to emerge as an important research tool in understanding nanoparticle uptake and their subsequent interactions within cells along with becoming a powerful developmental platform in the nascent field of NP-mediated drug delivery (NMDD).[14−19] The latter area seeks to overcome many of the issues associated with systemic delivery of high doses of toxic, relatively insoluble therapeutics by utilizing a biofunctionalized NP as a carrier coupled with a targeting agent to localize to tumors, for example. Successful development of NMDD is directly predicated on having available methods to specifically deliver QDs (and many other types of NP materials) to targeted intracellular compartments in a relatively facile manner. Delivery of QDs to a variety of cell and tissue types has already been demonstrated by using (1) passive delivery as exemplified by coincubation, which usually leads to pinocytosis; (2) facilitated delivery by using transfection reagents (i.e., Lipofectamine), mixing with "proton-sponge" chemicals such as polyethyleneimine or decorating the QDs with CPPs, antibodies, and other proteins/nutrients/cofactors primarily aimed at mediating endocytic uptake; and (3) active delivery methods such as electroporation, nucleofection, or microinjection, which can directly access the cytosol in some cases.[14−19] Despite the development of these various delivery regimes, it is important to note that the delivery of multiple different QD species to various targeted sites in the same cells or simultaneous incorporation of different delivery strategies still remains almost unexplored.

Here, we present an antibody-free, spaciotemporal strategy for the simultaneous, multicolor labeling of distinct intra- and extracellular compartments/structures in a live cellular system. This labeling approach exploits multivalent peptide display on QDs, FRET, and incorporates both innate cellular processes (peptide- and polymer-mediated endocytosis and receptor−ligand interactions) along with physical microinjection as QD delivery platforms (see schematic in Figure 1A). Our results demonstrate the utility of QDs as the basis of a multicolor labeling scheme for the robust targeting of intra- and extracellular targets without the need for bioconjugation to antibodies or cell permeabilization.

MATERIALS AND METHODS

Materials. DAPI nuclear stain and paraformaldehyde were obtained from Sigma (St. Louis, MO). PULSin was purchased from Polyplus-transfection (New York, NY). Dulbecco's Modified Eagle's Medium (DMEM) and fetal bovine serum were products of ATCC (Manassas, VA). Cell culture grade phosphate buffered saline (PBS) was from Invitrogen (Carlsbad, CA). All other materials were obtained as described.

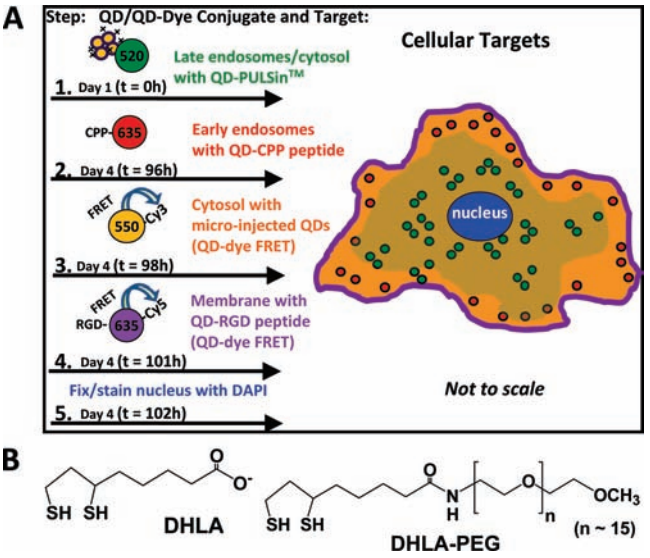

Figure 1. (A) Spatiotemporal strategy for multicolor QD labeling of A549 cells along with QD/QD−dye emissions utilized. Over a 4 day period, various cellular structures were labeled with different color QDs. Green 520 nm QDs were delivered on day 1 via PULSin to target late endosomes. After 4 days in culture, early endosomes were labeled by a 30 min incubation with 635 nm red QDs complexed with CPP. 550 nm QDs decorated with Cy3-labeled peptides for a yellow/orange FRET emission were then microinjected directly into the cytosol. 635 nm QDs assembled with Cy5-labeled peptides (far-red FRET emission) along with RGD peptides were used to bind integrin receptors and label the plasma membrane. After QD deliveries, cells were fixed and the nuclei stained with DAPI. (B) Structures of the QD capping ligands utilized to render the nanocrystals hydrophilic. QDs were rendered soluble using dihydrolipoic acid (DHLA) ligands modified with polyethylene glycol terminating in a methoxy group (DHLA-PEG, PEG MW ≈ 750). For the delivery of QDs with the cationic polymer PULSin, a mixed ligand surface was used bearing a net negative charge (consisting of 1:1 DHLA:DHLA-PEG) to allow for electrostatic assembly of the QD with the polymer. The DHLA is shown deprotonated, and the dithiols for both are in reduced form.

Quantum Dots and Capping Ligands. CdSe−ZnS core−shell QDs with emission maxima centered at 520, 550, 580, or 635 nm were synthesized and made hydrophilic by exchanging the native trioctylphosphine/trioctylphosphine oxide (TOP/TOPO) capping shell with either DHLA (dihydrolipoic acid) or polyethylene glycol (PEG)-appended DHLA ligands as described previously.[20,21] Ligand structures are presented in Figure 1B. Generally, PEGylated-QDs are preferred as they provide superior intracellular solubility and pH stability.[20−22] Late endosomes were labeled with 520 nm QDs capped with a 1:1 ratiometric mix of DHLA and DHLA-PEG ligands. Early endosomes were labeled with 635 nm QDs capped with DHLA-PEG ligands. The cytosol was labeled via microinjection of DHLA-PEG-capped 550 nm QDs appended with Cy3-labeled peptides (FRET configuration) or 580 nm QDs alone (non-FRET configuration). The plasma membrane was labeled with 635 nm QDs decorated with Cy5-labeled peptides, which also provide for FRET between the QD donor and dye acceptor.

Peptides. The cell-penetrating peptide (CPP, R_9GGLA(Aib)-SGWKH_6) used in this study is described in detail elsewhere.[23,24] This peptide consists of a C-terminal hexahistidine domain (H_6) for self-assembly of the peptide onto the QD surface and an N-terminal polyarginine domain (R_9) that mediates cellular uptake of the resulting conjugate. The two domains are separated by the spacer region consisting of the subsequence GGLA(Aib)SGWK. The RGD_3 peptide ([RGDSG]$_2$RGDGL AibA_3WGGH$_6$) used for the QD-labeling of membrane integrins is

Table 1. Peptide Sequences Used

Peptide:	Sequence:
CPP	$(Arg)_9$GlyGlyLeuAlaAibSerGlyTrpLys$(His)_6$
RGD	$(ArgGlyAspSerGly)_3$ArgGlyAspGlyLeuAib$(Ala)_3$TrpGlyGly$(His)_6$
Acceptor	Cys*GlySerGly$(Ala)_3$GlyLeuSer$(His)_6$

Aib = α-amino isobutyric acid. All N-terminal acetylated and C-terminal amidated. Functional peptide modules: cell uptake, membrane-binding, spacer, QD attachment and *dye-labeling-site.

composed of three "RGD" repeats also separated from the polyhistidine domain by a spacer sequence. In both peptides, Aib is the artificial residue α-amino isobutyric acid. For QD-peptide configurations in which the QD donor was engaged in FRET with an acceptor dye, a nonspecific acceptor peptide with the sequence $CGSGA_3GLSH_6$ (essentially cysteine-spacer-H_6) was labeled with Cy3- or Cy5-maleimide on the N-terminal cysteine residue. Peptide sequences are written in the conventional amino-to-carboxy terminus orientation; see Table 1. All peptides were synthesized using Boc-solid phase peptide synthesis, purified by HPLC, and characterized by electrospray ionization mass spectrometry. Peptides were labeled, purified, desalted, quantitated, and stored until use as described in detail in ref 25.

Cell Culture and Time-Resolved Multicolor Labeling of Live Cells with QDs. Adherent human alveolar adenocarcinoma cells (A549, ATCC, Manassas, VA) were used in this study as a model cell line because initial results demonstrated (1) their ability to endocytose QDs complexed with PULSin polymer or CPP, (2) their expression of $\alpha v\beta 3$ integrins (for labeling of the plasma membrane with RGD peptide-appended QDs), and (3) their amenability to microinjection. A549 cells have been frequently used for testing a variety of QD delivery regimes.[26,27] Cells were cultured in complete growth medium (DMEM) supplemented with 1% (v/v) antibiotic/antimycotic (Sigma) and 10% (v/v) heat inactivated fetal bovine serum (ATCC). Cells were cultured in T25 flasks and incubated at 37 °C under 5% CO_2 humidified atmosphere, and a subculture was performed every 3−4 days as described previously.[23,24]

Overview of Delivery Strategy. For multicolor labeling of cells with QDs, A549 cells were seeded (~1×10^4 cells/well) into 35 mm BD BioCoat coverslip-bottom dishes (BD Biosciences, Bedford, MA) coated with 5 μg/mL fibronectin (Sigma). On day one of the multiday delivery experiment, 520 nm QDs complexed with PULSin were incubated with the A549 cell monolayer for 2−3 h to mediate uptake of the QDs and labeling of the endocytic pathway. The QD-loaded cells were subsequently cultured for 3 days to allow a portion of the QDs to escape the late endosomes and enter the cytosol as reported previously.[23] On day four, the cell monolayer was washed with phosphate buffered saline (PBS, 137 mM NaCl, 10 mM phosphate, 3 mM KCl, pH 7.4) and the early endosomal pathway was labeled by briefly (30 min) incubating the cells with 100 nM 635 nm QDs appended with the CPP peptide (25 CPP/QD). The cell monolayer was washed again, and several fields of cells (approximately 20 cells per field) were microinjected with 550 nm QDs assembled with the nonspecific acceptor peptide labeled with Cy3 (3 peptides/QD). This allowed for FRET between the QD donor and the Cy3 dye acceptor (FRET configuration). In an alternative embodiment, several fields were injected with 580 nm QDs bearing no dye-labeled peptide (non-FRET configuration). Following microinjection, the cells were washed, and the plasma membrane was then labeled by incubating the cells for 20 min with 635 nm QDs (50 nM final concentration) assembled with RGD_3 peptides (20 RGD_3 peptides per QD) and a nonspecific Cy5-labeled peptide (4 peptides/QD) allowing for FRET between the QD and the Cy5 dye. The cells were then washed a final time, fixed with 3.7% paraformaldehyde in PBS (15 min), and the cell nuclei were counterstained with DAPI (2 μg/mL in PBS) prior to imaging.

PULSin-Mediated QD Delivery. A stock solution of 520 nm DHLA:DHLA-PEG QDs (1 μM in 0.1 M borate buffer, pH 8.9) was diluted to 0.5 μM in HEPES (4-(2-hydroxyethyl)-1-piperazineethanesulfonic acid, pH 8.2). PULSin delivery reagent was added (1 μL per 20 pmol QD), and complex formation was allowed to occur for 20 min at 25 °C. The complexes were diluted into serum free medium to a final QD concentration of 100 nM QD and incubated on the cells for 2−3 h at 37 °C. The complexes were removed, the cell monolayer was washed with PBS, and the cells were cultured in complete growth medium for 4 days prior to CPP-mediated QD delivery.

Table 2. Excitation Wavelengths and Spectral Emission Windows Used in This Study

laser (nm)	fluorophore	emission window	optical configuration
402	DAPI dye	410−430 nm	direct excitation
457	520 nm QD	510−530 nm	direct excitation
457	Cy3[a] acceptor dye	575−585 nm	550 nm QD donor/FRET
402	580 nm[b] QD	575−585 nm	direct excitation
457	635 nm QD	625−645 nm	direct excitation
457	Cy5[a] acceptor dye	691−730 nm	635 nm QD donor/FRET

[a] Cy3/Cy5 dyes are FRET-sensitized by indicated QD donors. [b] Alternate to Cy3.

Peptide-Mediated QD Delivery. To generate the indicated peptide-QD assemblies, peptide stocks were diluted into Dulbecco's Modified Eagle Medium (DMEM) supplemented with 25 mM HEPES ((DMEM/HEPES, pH 7.4), Invitrogen, Carlsbad, CA). An aliquot of stock QD solution was then added to the peptide solution at the appropriate molar ratio, and conjugate assembly proceeded for ~20 min. The QD−peptide complexes were incubated on the cell monolayer for 1 h followed by washing with PBS to remove unbound complexes.

Microinjection of QDs. Femtoliter volumes of DHLA-PEG-capped QDs were injected directly into the cytosol of A549 cells using an InjectMan NI2 micromanipulator equipped with a FemtoJet programmable microinjector (Eppendorf, Westbury, NY). During microinjection, the cells were maintained in DMEM/HEPES buffer (pH 7.4). Microinjection was performed on an Olympus IX-70 microscope equipped with a Microcode II Linear Measuring Stage (Boeckeler Instruments, Tucson, Arizona), and injected cells were periodically examined in fluorescence mode during the microinjection procedure to ensure successful QD loading and maintenance of plasma membrane integrity.

Microscopy and Image Analysis. Images were collected using a Nikon Eclipse TE2000-E confocal imaging system operated in epifluorescence mode. Excitation of samples was achieved with a 402 nm diode laser or a 457 argon laser. Differential interference contrast images (DIC) were collected using a bright light source. Excitation lines and the emission spectral windows used for each respective QD and QD−dye fluorophore emission are shown in Table 2. Imaging of both donor only control samples for the FRET configurations (no dye acceptor) showed no donor contribution in the acceptor channel under the image acquisition settings used (data not shown). Images were collected using Nikon NIS Elements software (ver. 2.3) and processed using Adobe PhotoShop CS2 (version 9.0).

Data Analysis. Solution-phase ensemble FRET data were collected using a Tecan Safire Dual Monochromator Multifunction Plate Reader (Tecan, Research Triangle Park, NC). Individual donor and acceptor emission spectra were deconvolved by comparison to control samples to provide the QD donor quenching and dye−acceptor sensitization components.[28] Experimentally, FRET efficiency E_n (where n is the ratio or valence of dye−acceptors per QD) was determined using:

$$E_n = \frac{(F_D - F_{DA})}{F_D} \quad (1)$$

where F_D and F_{DA} designate the fluorescence intensities of the donor alone and donor in the presence of acceptor(s), respectively.[28] Data from FRET efficiency were analyzed using Förster theory to determine values for center-to-center (QD-to-dye) separation distance r using eq 2, which assumes a centro-symmetric distribution of dye−acceptors

around a central QD:[28−30]

$$r = \left(\frac{n(1-E_n)}{E}\right)^{1/6} R_0 \quad (2)$$

R_0 designates the Förster distance corresponding to a FRET efficiency E of 50% for a single QD donor:single dye−acceptor ratio and is given by:

$$R_0 = 9.78 \times 10^3 [\kappa^2 \breve{n}^{-4} Q_D J(\lambda)]^{1/6} \quad (3)$$

where $\breve{n}$ is the refractive index of the medium, Q_D is the fluorescence quantum yield (QY) of the donor, $J(\lambda)$ is the spectral overlap integral, and κ^2 is the dipole orientation factor. We use a κ^2 value of 2/3, which is appropriate for the random dipole orientations found within these self-assembled configurations as described.[28−38] Because of the high FRET efficiencies measured for sample sets at relatively low ratios, heterogeneity in conjugate self-assembly valence was investigated and accounted for where applicable. This is accomplished by using a Poisson distribution function, $p(k,n)$, to describe the heterogeneity in conjugate valence where FRET E in eq 2 is further written as:

$$E(n) = \sum_{k=1}^{\infty} p(k,n)E(k) \text{ with } p(k,n) = \frac{e^{-n}n^k}{k!} \quad (4)$$

where n is the average acceptor-to-QD ratio used during reagent mixing, and k is the exact number of peptide−dye conjugated to the QD.[38]

RESULTS AND DISCUSSION

Delivery Strategy. The overall cellular delivery approach implemented here requires simultaneously exerting three levels of control over the materials and delivery process. These levels of control encompass: (1) QDs and bioconjugation to peptides, specifically incorporating multiple differentially emissive, pH-stable QDs with neutral or charged surfaces that are capable of displaying mixed peptide surfaces in a controlled manner; (2) QD emission and FRET, choosing a number of QD/QD−dye FRET pairs to provide a set of well-defined, spectrally separated, and easily resolvable emission windows; and (3) multistep cellular delivery, sequentially delivering different QD/QD−peptide conjugates to the same cell population via different techniques in a time-staggered manner.

Quantum Dots and Peptide Assembly. We utilize CdSe/ZnS core/shell QDs with distinct photoluminescence (PL) emission arrayed across the visible spectrum. The QDs are made soluble and pH stable using dihydrolipoic acid (DHLA) ligands modified with polyethylene glycol (PEG, MW ≈ 750) terminating in a methoxy group (DHLA-PEG).[32,33] For QDs requiring both pH stability and a net negative charge, we utilize a mixed ligand surface consisting of 1:1 DHLA:DHLA-PEG (see Figure 1B for chemical structures).[23] More pertinent to our needs, these QDs allow self-assembly of polyhistidine-(His_n) appended peptides via metal-affinity coordination between the QD's ZnS surface and the histidine's imidazolium side chains.[20,33−38] We, and several other groups, have shown that the His_n−QD interactions are rapid, equally applicable to a wide variety of commercial and other neutral or charged QDs, characterized by strong binding affinities, stable over a wide range of pH and intracellular environments, and allow for control over subsequent QD-biomolecular orientation.[20,33−38] We have further demonstrated that QDs can be controllably assembled with ratios ranging from 1 to 50 peptides along with providing access to mixed surfaces displaying multiple peptide species; each of the latter can also differ in valence assembled per QD if so required.[23,34,35] See Table 1 for the peptide sequences utilized where colors are used to highlight their common functional modularity.

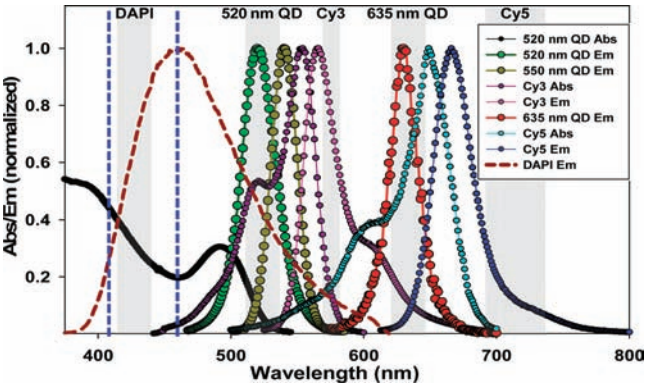

Figure 2. Spectral windows. Selected absorption and emission spectra of the QDs and dyes used in this study. DAPI, QD, and dye emission windows are shown in gray. DAPI excitation 405 nm and QD−dye excitation 457 nm are represented by blue dotted lines.

Quantum Dots and FRET. QDs have been repeatedly demonstrated as potent FRET donors, which can provide unique access to numerous photophysical properties that are cumulatively unavailable to organic dyes and fluorescent protein fluorophores when utilized in the same role.[6,10,12,28,35−38] Pertinent characteristics include the ability to: (1) select a QD PL maxima to optimize spectral overlap with a given acceptor; (2) excite a QD donor at a wavelength that corresponds to an acceptor absorption minima, thereby decreasing the direct acceptor excitation component; (3) array multiple dye-acceptors around the central QD in a centrosymmetrical fashion, which proportionally and controllably increases the acceptor absorption cross-section and increases the probability of FRET; and (4) realize multiplex FRET configurations in a relatively facile manner by incorporating multiple differentially emissive QDs engaged in FRET with different acceptors within the same sample format.[6,10,12,28,35−38] To address the current multicolor requirements, we utilize QDs alone and in combination with FRET sensitization of proximal dye-labeled acceptors to create a series of five increasingly red-shifted emission windows that range from 510 to 730 nm (see both Table 2 and Figure 2).

As shown in Figure 2, QD emission maxima at 520 and 635 nm provide two discrete PL windows. QDs are also utilized as antennas within two other bioconjugate configurations to sensitize acceptor dyes.[12] In the first conjugate, 550 nm QDs act as donors for sensitizing Cy3 acceptors ($\lambda_{abs.max.} \approx 550$ nm, $\varepsilon_c \approx 150\,000\ M^{-1}\ cm^{-1}$), while the same 635 nm QDs as above were coupled with Cy5 acceptors ($\lambda_{abs.max.} \approx 650$ nm, $\varepsilon_c \approx 250\,000\ M^{-1}\ cm^{-1}$); this gives rise to Förster distances (R_0) of 58.5 and 67.5 Å, respectively (see Materials and Methods for FRET analysis).[28,29] Collectively, this provides four distinct spectral windows while only requiring one excitation source at 457 nm to excite the QD samples. The fifth spectral window consists of the nuclear dye DAPI excited at 405 nm and monitored at <450 nm. To place acceptors in close proximity to the QD donor, we labeled the unique terminal-thiol on the acceptor peptide with maleimido-activated dye. The peptide is essentially a Cys-spacer-His_6 configuration designed specifically for labeling and ratiometric self-assembly onto QDs; its small size minimizes QD−dye separation.

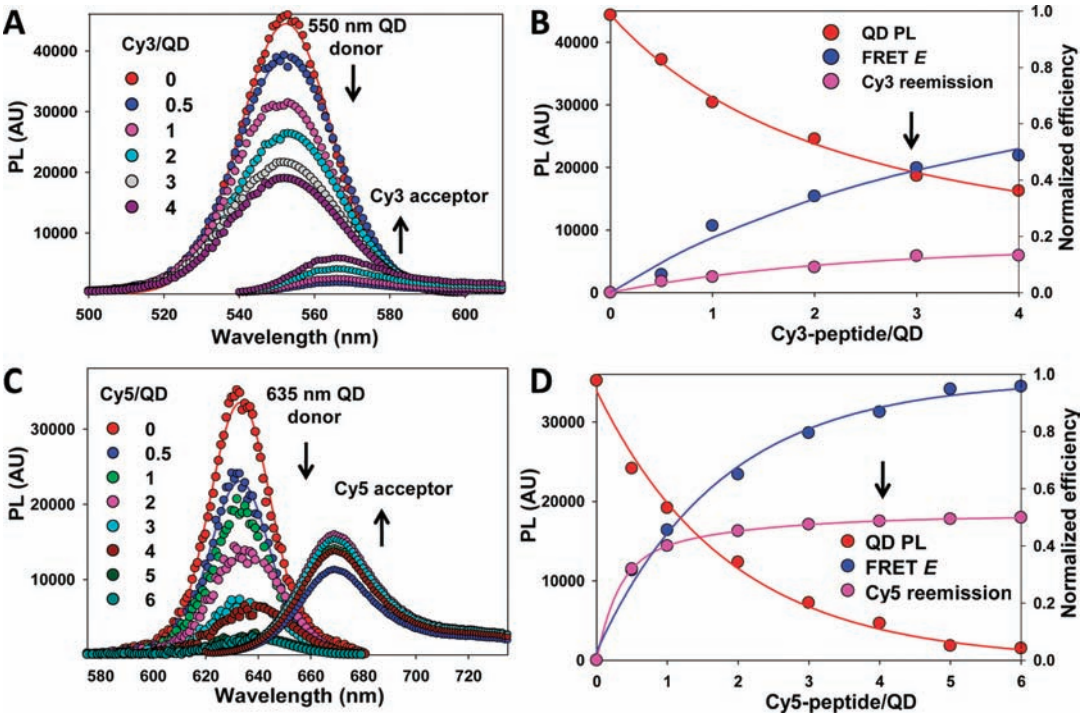

Figure 3. Spectra of QD donor−dye acceptor pairs. (A) Deconvoluted spectra of 550 nm QD donors (QY ≈ 0.2) assembled with Cy3-labeled acceptor peptide. Data corrected for Cy3 direct excitation. (B) Corresponding plots versus Cy3-acceptor/QD ratio of QD PL loss, FRET efficiency *E*, and Cy3-sensitization. Data were analyzed as described.[28−30,38] Data for FRET *E* are fitted on the basis of eq 4 and indicate very little deviation from the expected assembly kinetics. (C,D) Similar data for 635 nm QD donors (QY ≈ 0.4) with Cy5-acceptor labeled peptide. Arrows in (B,D) indicate ratios used in the cellular labeling.

To preoptimize sensitized signal from both of the cyanine acceptor dyes used here, we monitored FRET interactions as each QD donor was incrementally self-assembled with an increasing ratio of dye-labeled peptide in vitro (see Figure 3A−D). The unique ability to manipulate QD-peptide intraconjugate FRET via discrete self-assembly valence allows us the option of choosing acceptor/donor configurations for delivery of 3 Cy3/550 nm QD (FRET efficiency-*E* = 40%) and 4 Cy5/635 nm QD (FRET *E* = 90%). These represent ratios where QD donor PL is minimized and acceptor sensitization is enhanced. The high *E* of the latter donor−acceptor pair arises from a combination of high QD QY and Cy5's strong absorption. Optimization also limits QD donor PL bleed-through into acceptor channels. For example, in Figure 3A, examining the respective deconvoluted donor and acceptor PL curves in the evolution of solution-phase ensemble FRET data at 580 nm shows some overlap of the 550 nm QD donor and Cy3-acceptor emissions. In actual FRET imaging within cells (described below), we were only able to detect sensitized Cy3 emission in this spectral region. Although only a relatively modest Cy3 sensitized signal is present in this window, the ability to collect such emission over long time periods without fear of photobleaching allowed us to accomplish the necessary imaging. Importantly, PL from 550 nm QD-only control samples delivered to cells in the same manner could not be visualized with the same settings. However, we did note with these same control samples that if we shifted the emission window 20 nm to the blue (555−565 nm), 550 nm QD donor-only PL did start to have a significant contribution to this altered acceptor-monitoring channel (data not shown).

Multistep Cellular Delivery. QD delivery to eukaryotic cells has been repeatedly demonstrated with facilitated mechanisms such as transfection reagents or peptides along with active techniques such as electroporation or microinjection, although almost exclusively never in combination.[15,17,23,39,40] We recently showed that PULSin, a proprietary amphiphilic transfection polymer originally designed for cytosolic protein delivery, could mediate efficient cellular uptake of QDs. After 4−5 days in culture, a modest portion of the internalized QDs is released to the cytosol, while the majority of QDs remain sequestered within late endosomes, adopting what appeared to be a perinuclear morphology.[23] Our five-step delivery regime outlined in Figure 1 begins with endocytic delivery of 520 nm QDs capped with DHLA:DHLA-PEG using PULSin polymer to adherent A549 cells. The use of a mixed QD surface displaying the negatively charged DHLA allows for QD:polymer assembly. Following 4 days in culture, we next implemented peptide-mediated delivery to target the early endosomal pathway. To achieve this, 635 nm DHLA-PEG QDs were self-assembled with CPP at a ratio of ∼25 CPP/QD and incubated with the cells for 30 min. Endolysosomal vesicles can be specifically targeted for QD delivery by exploiting the HIV-derived polyarginine "TAT" peptidyl motif as an endocytic facilitator,[15,17,39,40] although some reports indicate significant exocytosis may occur over time.[40] The next step entailed microinjection of 550 nm DHLA-PEG QD donors self-assembled with 3-Cy3 acceptor-labeled peptides/QD directly into the cellular cytosol across several fields of view under a microscope, which required approximately 3 h. Following microinjection, another QD−dye pair was used to label the plasma membrane. For this, 635 nm QD donors were first assembled with 4-Cy5 acceptor-labeled peptides and then with 20 copies of the integrin-targeting RGD peptide and incubated with the cells for 20 min. This peptidyl motif targets $\alpha_V\beta_3$ integrin receptors displayed on the plasma membrane and its

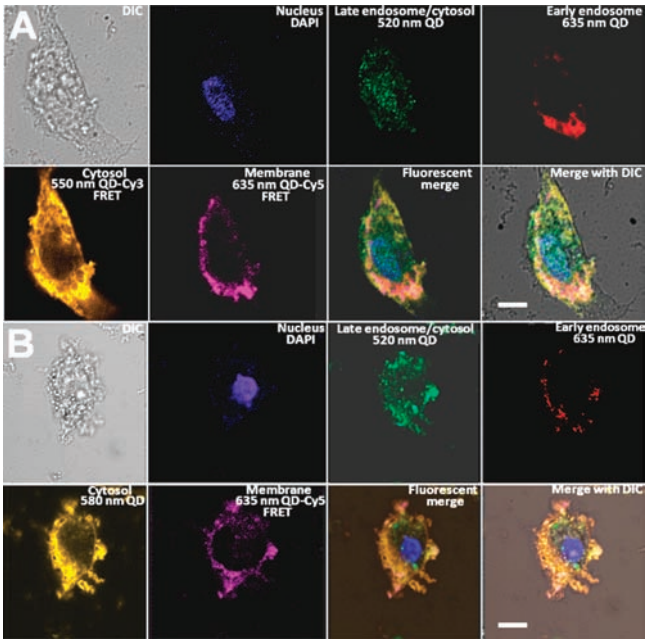

Figure 4. Representative image series of an A549 cell collected after sequential delivery of the indicated color QDs to specific cellular structures. Shown are the DIC along with the different fluorescent emissions from DAPI and the QD/QD-sensitized dye within each cellular compartment. Panel (A) corresponds to an image set from cells microinjected (cytosol) with QD−Cy3 conjugates engaged in FRET, while in panel (B) 580 nm QDs were injected into the cytosol yielding a non-FRET emission for that channel. The scale bar represents 5 μm. As indicated, the nuclei are DAPI stained (blue), late endosomes and the cytosol have 520 nm QDs present (green), early endosomes have 635 nm QDs present (red), the cytosol has 550 nm QD−Cy3 engaged in FRET or 580 nm QDs present (yellow), and membranes are labeled with 635 nm QD−Cy5 engaged in FRET (purple). False coloring is used to highlight the separate and distinct emissions.

binding interactions are potentiated when presented in a cyclic or repeated arrangement.[41,42] As these integrins are also up-regulated in many cancers, this same motif is commonly utilized for targeting QDs to the membranes of cancer cells.[34−36] Following QD delivery, the cells appeared visibly unperturbed for several hours, suggesting an available experimental window following labeling. The cells were then fixed, and the nuclei were counterstained with DAPI prior to imaging. Although fluorescence in cells could be (and was) directly imaged *in vivo* at this point, the cells were fixed for the purpose of maintaining consistent cellular morphology and labeling integrity, while the samples underwent detailed imaging and analysis over several days.

As highlighted in Figure 4A, this delivery regime results in cells that are labeled with five distinct fluorophores, four QDs (two engaged in FRET), and one nuclear stain, and these are imaged in six distinct spectral windows including DIC. The micrographs shown are representative of those collected from across several fields of microinjected cells. PL from the PULSin-delivered 520 nm QDs appeared as a mix of diffuse signal spread throughout the cytosol interspersed with more punctate signal. This is consistent with our previous findings where, after 4 days, we observed the escape of a small portion of the QDs to the cytosol, while the remainder stayed sequestered within late endosomes and displayed a punctate appearance.[23] The 635 nm QD-CPP displayed a largely punctate appearance that was localized primarily just inside the plasma membrane, consistent with localization in early endosomes and with previous QD delivery studies using this same peptidyl motif.[15,17,23,39,40] After microinjection, the 550 QD-peptide-Cy3 conjugates occupied the cellular cytosol and were excluded from the nucleus, confirming the intact nature of the nuclear and plasma membranes and QD dispersity. Final QD membrane labeling was achieved by incubating cells with 635 nm QD-RGD/Cy5-peptide. The resulting PL pattern was clearly membranous, indicative of the labeling of integrin receptors. Interestingly, piercing of the plasma membrane by microinjection did not appear to have a deleterious effect as integrin receptors were still able to interact with the RGD peptide on the QDs. Importantly, labeling specificity was as expected, consistent with previous results[15,17,23,39,40] and confirmed by control counterstaining (see Supporting Information Figure S1).

To evaluate the ability to modify emission colors or available fluorescent labeling channels in a facile manner, we repeated the same delivery/labeling methodology while changing the sample used for microinjection to 580 nm emitting QDs. In this non-FRET configuration, the QD is excited in the UV along with the other nanocrystals and emits directly in the center of the Cy3-acceptor channel (see Supporting Information Figure S2 for a schematic and the emission filter configuration). As shown in Figure 4B, an almost identical pattern of staining was obtained as the cytosol was again fully occupied by the QDs and excluded from the nucleus. These results also serve to highlight the inherent flexibility available in selecting and modifying different acquisition windows when working with QDs.

CONCLUSIONS

Here, we report a method for the facile delivery to and labeling of various distinct subcellular compartments using semiconductor nanocrystals within live cells without the need for cellular fixation/permeabilization. This strategy exploits the unique properties of QDs in conjunction with multiple innate and active/physical cellular delivery modalities over a 4 day period. Our results again lend credence to that concept that QD nanoparticles can provide multiple levels of utility for different types of cellular labeling. Their nontrivial surface areas, tunable ligand characteristics, and the ability to be controllably decorated with multiple peptides allow them to interact with both transfection reagents or directly with cell-membrane receptors in a high avidity configuration as needed. We note that the self-assembly bioconjugation chemistry utilized here is the most facile available and specific subcellular labeling is still achieved without requiring any antibodies. Further, the unique QD photophysical characteristics, in combination with their ability to function as versatile FRET donors, dramatically simplify imaging requirements and allow multiple spectral windows across the visible portion of the spectrum to be accessed with a single excitation wavelength. We also note that new emission channels can be created by simply pairing a dye−acceptor to the same QD color as may already be in use and tuning the FRET E to a level that allows for optimized imaging. Such FRET labeling configurations are also advantageous in that sensitized dyes are much less susceptible to photobleaching because they are not directly excited.

This approach does come with other inherent benefits and some liabilities. Exploiting cellular processes such as endocytosis or receptor−ligand binding with peptide- and PULSin-complexed QDs to facilitate labeling certainly eliminates the need

for cellular fixation and permeabilization. Understanding the intracellular fate of QD-bioconjugates over time in conjunction with staggered delivery steps allows for the targeting of specific subcellular structures and the optimization of labeling. For example, concerns about QD-CPP exocytosis over long time periods[40] resulted in utilizing this mechanism for labeling only early endosomes. Although applied separately, peptide- and PULSin-facilitated labeling of early/late endosomes and the membrane appeared relatively efficient with ~75% of cells displaying all three QD colors. Obviously, individually addressing cells by microinjection is the rate-limiting factor on the number of cells that are fully labeled with four QD colors. Another important concern is that of cellular toxicity. We have previously shown that the short exposure times used for QD-CPP delivery do not affect cellular viability.[15,23] In contrast, exposing cells to either PULSin alone or complexed to QDs reduces cell viability to <60%.[23] Clearly, reagent toxicity and cumulative delivery effects over time need to be carefully considered when implementing such approaches.

It is probable that the number of cellular compartments within live cells that could be labeled with this and similar types of delivery approaches can be expanded beyond the four demonstrated here. This would, however, require maintaining a judicious selection of QD or QD−dye acceptor emissions that are spectrally resolvable, which suggests expanding into the 700−850 nm portion of the near-IR spectrum. Beyond the delivery regimes utilized here, recent reports have suggested that QDs can be directly delivered to the cytosol or nucleus in certain circumstances through the use of appropriate peptide sequences.[14,15,18,23] It is likely that as additional targeting peptides are developed and tested, they may facilitate QD and nanoparticle delivery to other intracellular organelles such as the endoplasmic reticulum or mitochondria.[18,43] QDs labeled with these targeting peptides could then be appropriately incorporated as an added or simultaneous step within a similar time-staggered delivery protocol. In sum, the strategy presented here demonstrates that different delivery techniques can be combined to achieve specific labeling of cellular structures with QDs and suggests that similar approaches may be applicable with other complex combinations of nanoparticles and fluorescent materials in different cell lines.

■ ASSOCIATED CONTENT

Supporting Information. FRET analysis, alternate optical configuration, and further cellular imaging of controls. This material is available free of charge via the Internet at http://pubs.acs.org.

■ AUTHOR INFORMATION

Corresponding Author

james.delehanty@nrl.navy.mil; igor.medintz@nrl.navy.mil

Present Addresses

[||]Department of Chemistry and Biochemistry, Florida State University, Tallahassee, Florida 23306, United States.

■ ACKNOWLEDGMENT

We acknowledge DTRA/ARO, DARPA, NRL, and the NRL-NSI. C.E.B. and D.F. acknowledge NRC fellowships. J.B.B.-C. acknowledges a Marie Curie IOF.

■ REFERENCES

(1) Giepmans, B. N.; Adams, S. R.; Ellisman, M. H.; Tsien, R. Y. *Science* **2006**, *312*, 217–224.
(2) Dieterich, D. C. *Curr. Opin. Neurobiol.* **2010**, *20*, 623–630.
(3) Suzuki, T.; Matsuzaki, T.; Hagiwara, H.; Aoki, T.; Takata, K. *Acta Histochem. Cytochem.* **2007**, *40*, 131–137.
(4) Tsien, R. Y.; Miyawaki, A. *Science* **1998**, *280*, 1954–1955.
(5) *The Handbook: A Guide to Fluorescent Probes and Labeling Technologies*, 10th ed.; Haugland, R., Ed.; Invitrogen: San Diego, CA, 2005.
(6) Sapsford, K. E.; Berti, L.; Medintz, I. L. *Angew. Chem., Int. Ed.* **2006**, *45*, 4562–4589.
(7) Schrock, E.; du Manoir, S.; Veldman, T.; Schoell, B.; Wienberg, J.; Ferguson-Smith, M. A.; Ning, Y.; Ledbetter, D. H.; Bar-Am, I.; Soenksen, D.; Garini, Y.; Ried, T. *Science* **1996**, *273*, 494–497.
(8) Hsu, F. D.; Nielsen, T. O.; Alkushi, A.; Dupuis, B.; Huntsman, D.; Liu, C. L.; van de Rijn, M.; Gilks, C. B. *Mod. Pathol.* **2002**, *15*, 1374–80.
(9) Ligler, F. S.; Taitt, C. R.; Shriver-Lake, L. C.; Sapsford, K. E.; Shubin, Y.; Golden, J. P. *Anal. Bioanal. Chem.* **2003**, *377*, 469–477.
(10) Algar, W. R.; Krull, U. J. *Anal. Bioanal. Chem.* **2010**, *398*, 2439–2449.
(11) Klostranec, J. M.; Chan, W. C. W. *Adv. Mater.* **2006**, *18*, 1953–1964.
(12) Medintz, I. L.; Mattoussi, H. *Phys. Chem. Chem. Phys.* **2009**, *11*, 17–45.
(13) Resch-Genger, U.; Grabolle, M.; Cavaliere-Jaricot, S.; Nitschke, R.; Nann, T. *Nat. Methods* **2008**, *5*, 763–765.
(14) Delehanty, J. B.; Boeneman, K.; Bradburne, C. E.; Robertson, K.; Bongard, J. E.; Medintz, I. L. *Ther. Delivery.* **2010**, *1*, 411–433.
(15) Delehanty, J. B.; Mattoussi, H.; Medintz, I. L. *Anal. Bioanal. Chem.* **2009**, *393*, 1091–1105.
(16) Delehanty, J. B.; Boeneman, K.; Bradburne, C. E.; Robertson, K.; Medintz, I. L. *Expert Opin. Drug Delivery* **2009**, *6*, 1091–1112.
(17) Biju, V.; Itoh, T.; Ishikawa, M. *Chem. Soc. Rev.* **2010**, *39*, 3031–3056.
(18) Fonseca, S. B.; Pereira, M. P.; Kelley, S. O. *Adv. Drug Delivery Rev.* **2009**, *61*, 953–964.
(19) Paleos, C. M.; Tziveleka, L. A.; Sideratou, Z.; Tsiourvas, D. *Expert Opin. Drug Delivery* **2009**, *6*, 27–38.
(20) Mei, B. C.; Susumu, K.; Medintz, I. L.; Delehanty, J. B.; Mountziaris, T. J.; Mattoussi, H. *J. Mater. Chem.* **2008**, *18*, 1–11.
(21) Mattoussi, H.; Mauro, J. M.; Goldman, E. R.; Anderson, G. P.; Sundar, V. C.; Mikulec, F. V.; Bawendi, M. G. *J. Am. Chem. Soc.* **2000**, *122*, 12142–12150.
(22) Susumu, K.; Uyeda, H. T.; Medintz, I. L.; Pons, T.; Delehanty, J. B.; Mattoussi, H. *J. Am. Chem. Soc.* **2007**, *129*, 13987–13996.
(23) Delehanty, J. B.; Bradburne, C. E.; Boeneman, K.; Susumu, K.; Farrell, D.; Mei, B. C.; Blanco-Canosa, J. B.; Dawson, G.; Dawson, P. E.; Mattoussi, H.; Medintz, I. L. *Integr. Biol.* **2010**, *2*, 265–277.
(24) Delehanty, J. B.; Medintz, I. L.; Pons, T.; Brunel, F. M.; Dawson, P. E.; Mattoussi, H. *Bioconjugate Chem.* **2006**, *17*, 920–927.
(25) Sapsford, K. E.; Farrell, D.; Steven Sun, S.; Rasooly, A.; Mattoussi, H.; Medintz, I. L. *Sens. Actuators, B* **2009**, *139*, 13–21.
(26) Song, E. Q.; Zhang, Z. L.; Luo, Q. Y.; Lu, W.; Shi, Y. B.; Pang, D. W. *Clin. Chem.* **2009**, *55*, 955–963.
(27) Ulasov, A. V.; Khramtsov, Y. V.; Trusov, G. A.; Rosenkranz, A. A.; Sverdlov, E. D.; Sobolev, A. S. *Mol. Ther.* **2011**, *19*, 103–112.
(28) Clapp, A. R.; Medintz, I. L.; Mauro, J. M.; Fisher, B. R.; Bawendi, M. G.; Mattoussi, H. *J. Am. Chem. Soc.* **2004**, *126*, 301–310.
(29) Lakowicz, J. R. *Principles of Fluorescence Spectroscopy*, 3rd ed.; Springer: New York, 2006.
(30) Dennis, A. M.; Sotto, D. C.; Mei, B. C.; Medintz, I. L.; Mattoussi, H.; Bao, G. *Bioconjugate Chem.* **2010**, *21*, 1160–1170.
(31) Pons, T.; Uyeda, H. T.; Medintz, I. L.; Mattoussi, H. *J. Phys. Chem. B* **2006**, *110*, 20308–20316.

(32) Mei, B. C.; Susumu, K.; Medintz, I. L.; Mattoussi, H. *Nat. Protoc.* **2009**, *4*, 412–423.
(33) Liu, W.; Howarth, M.; Greytak, A. B.; Zheng, Y.; Nocera, D. G.; Ting, A. Y.; Bawendi, M. G. *J. Am. Chem. Soc.* **2008**, *130*, 1274–1284.
(34) Sapsford, K. E.; Pons, T.; Medintz, I. L.; Higashiya, S.; Brunel, F. M.; Dawson, P. E.; Mattoussi, H. *J. Phys. Chem. C* **2007**, *111*, 11528–11538.
(35) Prasuhn, D. E.; Deschamps, J. R.; Susumu, K.; Stewart, M. H.; Boeneman, K.; Blanco-Canosa, J. B.; Dawson, P. E.; Medintz, I. L. *Small* **2010**, *6*, 555–564.
(36) Dennis, A. M.; Bao, G. *Nano Lett.* **2008**, *8*, 1439–1445.
(37) Yao, H.; Zhang, Y.; Xiao, F.; Xia, Z.; Rao, J. *Angew. Chem., Int. Ed.* **2007**, *46*, 4346–4349.
(38) Pons, T.; Medintz, I. L.; Wang, X.; English, D. S.; Mattoussi, H. *J. Am. Chem. Soc.* **2006**, *128*, 15324–15331.
(39) Derfus, A. M.; Chan, W. C. W.; Bhatia, S. N. *Adv. Mater.* **2004**, *16*, 961–966.
(40) Jiang, X.; Rocker, C.; Hafner, M.; Brandholt, S.; Dorlich, R. M.; Nienhaus, G. U. *ACS Nano* **2010**, *4*, 6787–6797.
(41) Hersel, U.; Dahmen, C.; Kessler, H. *Biomaterials* **2003**, *24*, 4385–4415.
(42) Auzzas, L.; Zanardi, F.; Battistini, L.; Burreddu, P.; Carta, P.; Rassu, G.; Curti, C.; Casiraghi, G. *Curr. Med. Chem.* **2010**, *17*, 1255–1299.
(43) Sawant, R.; Torchilin, V. *Mol. BioSyst.* **2010**, *6*, 628–640.